First-principles calculations of bulk and interfacial thermodynamic properties for fcc-based Al-Sc alloys

Mark Asta, S. M. Foiles, and A. A. Quong*
Computational Materials Sciences Division, Sandia National Laboratories, P.O. Box 969, MS 9161, Livermore, California 94551-0969
(Received 17 November 1997)

The configurational thermodynamic properties of fcc-based Al-Sc alloys and coherent Al/Al_3Sc interphase-boundary interfaces have been calculated from first principles. The computational approach used in this study combines the results of pseudopotential total-energy calculations with a cluster-expansion description of the alloy energetics. Bulk and interface configurational-thermodynamic properties are computed using a low-temperature-expansion technique. Calculated values of the {100} and {111} Al/Al_3Sc interfacial energies at zero temperature are, respectively, 192 and 226 mJ/m^2. The temperature dependence of the calculated interfacial free energies is found to be very weak for {100} and more appreciable for {111} orientations; the primary effect of configurational disordering at finite temperature is to reduce the degree of crystallographic anisotropy associated with calculated interfacial free energies. The first-principles-computed solid-solubility limits for Sc in bulk fcc Al are found to be underestimated significantly in comparison with experimental measurements. It is argued that this discrepancy can be largely attributed to nonconfigurational contributions to the entropy which have been neglected in the present thermodynamic calculations.
[S0163-1829(98)06518-7]

I. INTRODUCTION

The formation of second-phase precipitates is a commonly used method for strengthening metallic alloys. The Al-Sc alloy system provides a good model system for the study of precipitate formation via the process of homogeneous nucleation. The features which make this system desirable are that in supersaturated Al alloys aged between temperatures of 561 and 616 K: nucleation of the Al_3Sc phase is experimentally observed to be predominantly homogeneous, the precipitates are well-ordered coherent and spherical, and well characterized experimental observations of the precipitation kinetics have been performed.[1,33] A crucial parameter that influences the precipitation kinetics is the interfacial free energy between the precipitate phase and the matrix phase, in this case $L1_2$ Al_3Sc and fcc Al, respectively. The goal of the current work is to determine the excess configurational free energy of the coherent Al/Al_3Sc interface as a function of temperature and crystallographic orientation. To this end the zero-temperature interfacial energy and relaxed atomic structure of the interphase-boundary interface between Al and Al_3Sc are computed from first principles. To address the finite-temperature configurational-thermodynamic properties, a cluster expansion[2] is developed for the energetics of ordered and disordered fcc-based Al-Sc alloys. The interaction parameters in this expansion are derived from first-principles-calculated formation energies for a large number of relaxed fcc-based crystal structures with relatively small unit cells. The cluster expansion for the energy is used in a low-temperature-expansion (LTE) calculation in order to obtain the compositional variations at the coherent Al/Al_3Sc interphase boundary and the finite-temperature interfacial free energy. In this study we are concerned only with coherent Al/Al_3Sc interfaces; the lattice parameters of fcc Al and $L1_2$ Al_3Sc differ by only 1% (Ref. 3) and Al_3Sc precipitates remain coherent up to particle sizes of 20–30 nm.[4]

In previous experimental work, the nucleation kinetics for Al_3Sc precipitation in supersaturated Al-Sc alloys were measured by Hyland.[1] This data was analyzed in terms of classical nucleation theory and an Al/Al_3Sc interfacial free energy of 94 ± 23 mJ/m^2 was deduced in the temperature range between 561 and 616 K. Jo and Fujikawa[33] measured coarsening kinetics for Al_3Sc precipitates and obtained estimates of the interfacial free energy between 40 and 60 mJ/m^2 in the temperature range of 643–733 K. In addition, there has been some atomic-scale modeling of this interface based on the embedded-atom method (EAM) by Hyland *et al.*[5] In this work, the zero-temperature interfacial energies were computed to be 33, 51, and 78 mJ/m^2 for {100}, {110}, and {111} interfaces, respectively. Finite-temperature effects were investigated using both LTE and Monte Carlo simulation techniques. It was found that the temperature dependence of the {100} interfacial free energy was relatively weak below the melting point of Al, yet there is appreciable interface diffuseness at finite temperatures with the composition varying between the Al and Al_3Sc phases over roughly four atomic planes. Due to the differences between experimental estimates and the EAM values of the interfacial energy, it is worthwhile to obtain an independent estimate based upon first-principles calculations.

An additional goal of this work is to examine the accuracy of some of the methods used in the first-principles calculations. First, the predictive capabilities of the cluster expansion are studied in detail. We examine the accuracy of predictions for the zero-temperature interfacial energies and Sc dilute heat of solution for a number of different cluster expansions including successively larger sets of interaction parameters. From these results we determine the range of interactions required to represent accurately the interfacial

energetics and alloy thermodynamics. The electronic-structure calculations in this paper are performed using a pseudopotential methodology. The accuracy of the pseudopotentials for Al-Sc alloys is assessed by comparing energies and structural parameters for some simple crystal structures obtained from both pseudopotential and all-electron, full-potential electronic-structure calculations.

This paper is organized as follows. The next section describes the details of the computational methods. In the third section we present results for the structural and energetic properties of bulk fcc-based Al-Sc alloys and Al/Al_3Sc interfaces at zero temperature. An analysis of the predictive capabilities of the cluster expansion and the accuracy of the pseudopotentials are then discussed. In the fourth section we present results of finite-temperature calculations for configurational thermodynamic properties. In the last section our results are compared to those of previous theoretical and experimental work for Al/Al_3Sc interfaces as well as for related fcc/$L1_2$ interphase boundaries in the Al-Li alloy system.

II. COMPUTATIONAL METHODS

A. Pseudopotential calculations

Total energies of Al-Sc fcc-based compounds and Al/Al_3Sc interfacial energies have been calculated using a mixed-basis pseudopotential approach.[6] The basis set used in these electronic-structure calculations included both plane waves and pseudoatomic wave functions. A 5 Ry cutoff was used for the plane-wave basis set. Al and Sc s, p, and d pseudoatomic wave functions were included in the basis set. These local wave functions were represented in reciprocal space using a cutoff of 50 Ry. All electronic-structure calculations were performed using the Ceperly-Alder exchange-correlation potential as parametrized by Perdew and Zunger.[7] Reciprocal-space summations were performed by the method of special points[8] with sufficient numbers of **k** points to ensure that energy differences were converged to within a few percent. For Sc and Al we used optimized[9,10] and Troullier-Martins[11] pseudopotentials, respectively.

B. All-electron calculations

In order to test the accuracy of the pseudopotentials used in the present study, we performed several benchmark calculations based upon the all-electron, full-potential-linear-augmented-plane-wave (FLAPW) method.[12,13] As in the pseudopotential work, all FLAPW calculations were performed using the Perdew-Zunger parametrization for the exchange-correlation potential.[7] For Sc the $3p$ (and to a lesser extent the $3s$) core electrons lie at energies which are relatively close to the valence bands and they can display non-negligible dispersion in crystalline solids. For this reason we have treated the Sc $3s$ and $3p$ ''semicore'' states in a manner equivalent to the valence states by including them in the FLAPW basis set using lower values of the linearization energies.[13]

C. Cluster expansion

For the purpose of performing configurational-thermodynamic calculations in the present study we made use of a cluster-expansion description[2] of the energetics of fcc-based Al-Sc alloys. In particular, we used the formulation of the cluster expansion due to Laks *et al.*[14] Within this formulation the total energy of any arrangement (σ) of Al and Sc atoms on an fcc lattice can be written as follows:

$$E(\sigma)=N\sum_{\mathbf{k}} J(\mathbf{k},c)|S(\mathbf{k})|^2 + \left\{ E_0+\sum_{\mathbf{p}} E_{\mathbf{p}}\sigma_{\mathbf{p}}+\frac{1}{2}\sum_{\mathbf{p},\mathbf{p}'} E_{\mathbf{p},\mathbf{p}'}\sigma_{\mathbf{p}}\sigma_{\mathbf{p}'}+\ldots \right\}. \quad (1)$$

In Eq. (1) σ_p is an occupation variable which takes on values of $+1$ or -1 if a Sc or Al atom is associated with fcc lattice site **p**, respectively, $S(\mathbf{k})$ represents the Fourier transform of $S(\mathbf{p}-\mathbf{p}')=\sigma_{\mathbf{p}}\sigma_{\mathbf{p}'}$, and N is the number of lattice sites. The first term on the right-hand side of Eq. (1) represents the elastic-strain energy associated with size differences between the constituent atoms in the alloy.[14] The interaction parameter $J(\mathbf{k},c)$ is composition dependent, vanishes at the origin $(\mathbf{k}=0)$, and depends only upon direction in reciprocal space (i.e., it is independent of the magnitude of the **k** vector along a particular direction). Laks *et al.* derived an expression for $J(\mathbf{k},c)$ which is formulated in terms of the elastic constants of the elemental constituents within linear anisotropic elasticity theory.[14] In the present work the appropriate ratios of elastic constants arising in this formulation were calculated using the pseudopotential approach described above.

The term in brackets on the right-hand side of Eq. (1) is the cluster expansion for the ''chemical'' and relaxation energies.[14,15] In the present work this term is written in real space as a sum over points, pairs, triplets, etc., of lattice points. Each term in the brackets of Eq. (1) is written in terms of effective cluster interaction (ECI) parameters (e.g., $E_{\mathbf{p},\mathbf{p}'}$) and products of spin variables (e.g., $\sigma_{\mathbf{p}},\sigma_{\mathbf{p}'}$) referred to as cluster functions.[2] The ECI's parametrize changes in the total energy resulting from atomic rearrangements. The values of these parameters were obtained by fitting Eq. (1) to the total energies of pseudopotential-calculated, fcc-based ordered superstructures. Specifically, the total energies of 20 ordered superstructures were calculated, allowing for complete structural relaxations. From the total energy of each fully relaxed superstructure, the strain energy [first term in Eq. (1)] was subtracted. The cluster expansion was then fit to the resulting energy differences. A number of fits were performed retaining different sets of ECI's. The expansion for the energy was considered to be sufficiently accurate for the present work when the values of the Al/Al_3Sc energies and Sc heats of solution predicted by Eq. (1) agreed to within approximately 10% of the directly calculated values (roughly the accuracy of the pseudopotential calculations). Further details concerning the set of interaction parameters used in this study will be given below.

It should be emphasized that for the purposes of the present study, in which we are interested in coherent interfaces, it is essential to include the first term on the right-hand side of Eq. (1) due to the contribution to the energy arising from elastic coherency strains. In particular, consider the case where a coherent interface exists between two semi-infinite phases with different lattice parameters. An elastic-strain-energy contribution to the total energy of such an inhomogeneous system arises due to the fact that each phase

must be strained owing to the constraint of coherency at the interface. This strain energy scales with the volume of each phase in general. However, if the total energy of such an inhomogeneous system is described by a cluster expansion containing interaction parameters within a finite range, it will be found that the excess energy (relative to the bulk unstrained phases) scales with the area of the interface, not the volume of the strained phases. In other words, the coherency-strain energy cannot be properly described by a cluster expansion with finite-ranged interactions. This failing of the traditional cluster-expansion description for the energy was originally pointed out by Laks *et al.*[14] for long-period superlattices. These authors showed that the first term in Eq. (1) corrects the problem and provides the correct asymptotic value of the excess energy for large superlattices, as given by linear anisotropic elasticity theory.

D. Low-temperature expansion

The primary goal of this work is to calculate the finite-temperature thermodynamic properties of the coherent Al/Al_3Sc interface, including configurational entropy contributions to the interfacial free energy. For this purpose LTE calculations of finite-temperature grand potentials (Ω) (Ref. 16) were performed for the bulk Al and Al_3Sc phases, as well as for {100} and {111} Al/Al_3Sc interfaces. In the LTE method (see, for example, Ref. 17), Ω is calculated directly from a Taylor-series expansion of the logarithm of the alloy partition function. To second-order, the LTE expression for the grand-potential has the following form:

$$\Omega(\Delta\mu,T)=\Omega(\Delta\mu,\ T=0)-k_BT\sum_{\mathbf{p}}\ \exp(-\Delta\omega_{\mathbf{p}}/k_BT)$$
$$+\frac{1}{2}\,k_BT\sum_{\mathbf{p}}\ \exp(-2\Delta\omega_{\mathbf{p}}/k_BT)$$
$$-\frac{1}{2}\,k_BT\sum_{\mathbf{p},\mathbf{p}'}\ \{\exp(-\Delta\omega_{\mathbf{p},\mathbf{p}'}/k_BT)$$
$$-\exp[-(\Delta\omega_{\mathbf{p}}+\Delta\omega_{\mathbf{p}'})/k_BT]\},\qquad(2)$$

where the sums are over lattice sites $\mathbf{p}$ and $\mathbf{p}'$ ($\mathbf{p}\neq\mathbf{p}'$) and where k_B and T represent Boltzmann's constant and the temperature, respectively. In Eq. (2), $\Delta\mu$ is the chemical field, defined in terms of the difference between the chemical potentials for Al and Sc. $\Omega(\Delta\mu,\ T=0)$ represents the zero-temperature grand potential, and the variables $\Delta\omega_{\mathbf{p}}$ and $\Delta\omega_{\mathbf{p},\mathbf{p}'}$ represent configurational *excitation energies*. $\Delta\omega_{\mathbf{p}}$ denotes the change in the zero-temperature grand potential associated with switching the atom type at site $\mathbf{p}$. Similarly, $\Delta\omega_{\mathbf{p},\mathbf{p}'}$ is the cost in the zero-temperature grand potential associated with changing atom types at both sites $\mathbf{p}$ and $\mathbf{p}'$.

The LTE approach is appropriate when the excitation energies are large compared to the temperature and when all of the low lying excitations correspond to atomic rearrangements involving a small number of atoms. In other words, the LTE approach is appropriate when there are no low-energy excitations involving cooperative changes of a number of atoms greater than the size of the largest cluster considered in the expansion, in this case two. As will be discussed in detail below, the LTE approach was found to provide highly accurate configurational-thermodynamic properties in this study.

Formally, the finite-temperature interfacial free energy for an interface with orientation (hkl) can be written as follows:[16] $\gamma_{hkl}(T)=[\Omega_{hkl}(\Delta\mu_0,T)-\Omega_0(\Delta\mu_0,T)]/A$, where Ω_{hkl} is the value of the grand potential for an inhomogeneous alloy system containing an (hkl)-oriented interface, and Ω_0 corresponds to the *elastically distorted* (due to coherency strains) homogeneous bulk phases. The values of the grand potentials in this definition for γ_{hkl} are evaluated at $\Delta\mu_0$, the chemical field for which the elastically distorted bulk phases are in chemical equilibrium. Using the LTE approach, the relevant grand-potential values required to calculate $\gamma_{hkl}(T)$ can be determined once the excitation energies have been computed for all symmetry-inequivalent points in the bulk phases, and for all points inside a region near the interphase boundary where $\Delta\omega_{\mathbf{p}}$ and $\Delta\omega_{\mathbf{p},\mathbf{p}'}$ differ from the corresponding values in the bulk phases.

In the present work we use the cluster expansion, Eq. (1), for the purpose of calculating the values of the excitation energies. In calculating the strain-energy contributions to $\Delta\omega_{\mathbf{p}}$ and $\Delta\omega_{\mathbf{p},\mathbf{p}'}$ we employed an approximation whereby the isotropic form of the first term in Eq. (1) was used. This approximation was found to be highly accurate for the Al-rich alloys studied here. In order to compute the ''chemical'' and relaxation-energy contributions to the excitation energies, the changes in the values of the cluster functions [products of spin variables appearing in the bracketed term in Eq. (1)] arising from atomic rearrangements were determined by evaluating the differences in the products of spin variables associated with ordered and disordered supercells for each of the $L1_2$ (Al_3Sc), fcc (Al), and fcc/$L1_2$ (interface) structures.

III. ZERO-TEMPERATURE ENERGETICS AND STRUCTURAL PROPERTIES

A. Energies of fcc superstructures

In order to determine the parameters in the cluster expansion, Eq. (1), the energies of a large number of fcc-based superstructures were computed. The results of these calculations are listed in Table I and descriptions of the structures can be found in Refs. 15 and 18. Full structural relaxations were performed in the energy calculations for all structures listed in Table I. This includes adjusting the volume per atom as well as any distortions of the structure, such as c/a ratios, and relaxation of any internal degrees of freedom. The formation energies (ΔE) reported in Table I are computed relative to the fcc phases of both Al and Sc.

In the experimentally assessed Al-Sc phase diagram[19] $L1_2Al_3Sc$ is the only fcc-based superstructure phase. Unfortunately, we are not aware of any experimental results for the heat of formation (ΔH) for this phase. However, in our calculations we find that the energies of the $L1_0$ and $B2$ structures for AlSc are essentially equal. $B2$ is the experimentally observed structure for the stable AlSc phase[19] and its heat of formation has been measured to be -0.43 eV/atom.[20] This number compares favorably with our calculated value of

TABLE I. Calculated values of the formation energies (ΔE) and atomic volumes (V) for fcc-based superstructures of Al-Sc. Formation energies are defined with respect to the energies of fcc Al and Sc. The values of ΔE in the second column were obtained using fully relaxed energies for compounds. For a description of structures α, β, X, and $Z2$ see Ref. 15, and references therein; other structures are shown in Ref. 18.

Compound; Structure	ΔE (eV/atom)	V (Å^3/atom)
Al; fcc	0.000	15.5
Al_8Sc; Pt_8Ti prototype	−0.113	16.2
Al_4Sc; $D1_a$	−0.225	16.6
Al_3Sc; $L1_2$	−0.482	16.3
Al_3Sc; DO_{22}	−0.382	16.8
Al_3Sc; X	−0.295	17.0
Al_2Sc; β	−0.265	17.4
Al_2Sc; α	−0.089	17.9
AlSc; $L1_0$	−0.483	18.3
AlSc; $L1_1$	−0.249	19.6
AlSc; A_2B_2 40	−0.334	18.9
AlSc; A_2B_2 $Z2$	−0.255	18.8
$AlSc_2$; β	−0.341	20.0
$AlSc_2$; α	−0.151	20.6
$AlSc_3$; $L1_2$	−0.300	20.3
$AlSc_3$; DO_{22}	−0.255	20.4
$AlSc_3$; X	−0.173	20.8
$AlSc_4$; $D1_a$	−0.183	20.9
$AlSc_8$; Pt_8Ti prototype	−0.101	21.9
Sc; fcc	0.000	22.9

$\Delta H = -0.46$ eV/atom at zero temperature (unlike the values of ΔE listed in Table I, this value of ΔH is referenced to fcc Al and hcp Sc).

The values of ΔE for fcc-based Al-Sc structures are plotted versus concentration in Fig. 1. The solid lines connect

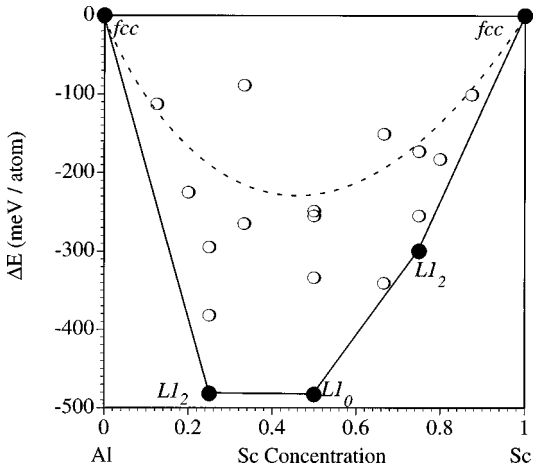

FIG. 1. Calculated formation energies for the fcc-based superstructures listed in Table II versus Sc concentration. Ground-state structures are indicated by filled symbols and formation energies for all other metastable structures are plotted by open circles. The solid line connects ground-state structures and the dashed line corresponds to the formation energies of random, disordered fcc alloys as computed by the cluster expansion (see text).

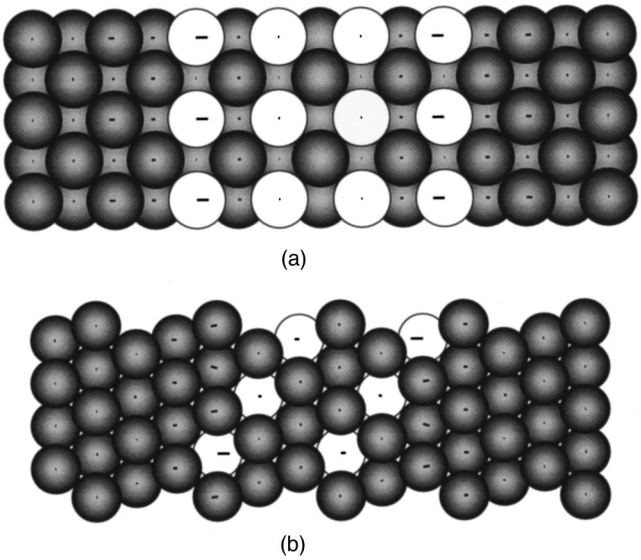

FIG. 2. Structures of the supercells used in the calculation of (a) {100} and (b) {111} interfacial energies. Black and white circles denote Al and Sc atoms, respectively. The lines indicate the displacement from the original (unrelaxed) atomic positions magnified by a factor of 10.

those structures listed in Table I which are found to be fcc ground states (i.e., they are lower in energy than all other fcc-based structures considered at the same composition and they are stable with respect to phase separation to any pair of the other structures considered). Of the structures listed in Table I, only $L1_0$ AlSc and $L1_2$ Al_3Sc and $AlSc_3$ are predicted to be fcc ground states. Monte Carlo simulations were performed at 600 K using a cluster expansion containing pair interactions out to eighth neighbor, triplet interactions out to fourth neighbor, and four-body interactions out to second neighbor (see below). In these simulations, which were performed in the grand-canonical ensemble as a function of chemical field ($\Delta\mu$), only five fcc-based phases were observed which included the two solid-solution phases, the $L1_0$ and the two $L1_2$ ordered phases. This result is consistent with the experimental phase diagram which shows only the Al and Al_3Sc fcc-based phases to be stable between 0 and 66 at. % Sc (for larger Sc concentrations there only non-fcc-based phases observed experimentally). Also consistent with the experimental phase diagram, which features a highly stable $L1_2$ Al_3Sc phase, the $L1_2$ structure is shown to have a negative formation energy which is very large in magnitude at the Al_3Sc composition in Fig. 1. The dashed line in Fig. 1 corresponds to the formation energy for the random disordered fcc solid-solution phase which was computed from the same cluster expansion as was used in the Monte Carlo simulations. The ordering energy for the $L1_2$ Al_3Sc phase (defined as the difference between the energies for the random alloy and the ordered phase at the same composition) is calculated to be 0.29 eV/atom. This relatively large value is consistent with the experimental observation that the ordered Al_3Sc phase remains highly ordered up to its melting point.[21]

B. Coherent Al/Al_3Sc interfaces

The zero-temperature interfacial energies and relaxed interphase-boundary atomic structures were computed di-

rectly (i.e., not from the cluster expansion) for two different crystallographic orientations (100) and (111). Interfacial energies were computed using periodic cells with alternating layers of Al and Al_3Sc as shown in Figs. 2(a) and 2(b). These geometries thus contain arrays of interfaces. The lattice constant in the plane of the interface was chosen to correspond to the value calculated for bulk fcc Al. Due to this choice, the Al_3Sc phase is distorted in the direction perpendicular to the interface due to the Poisson effect. This distortion was computed by minimizing the energy of an Al_3Sc cell where either a (100) or (111) plane is constrained to have the Al lattice constant. The resulting out-of-plane strains were computed to be 2.0 and 2.6 % for the (100) and (111) cells, respectively. This distortion can also be computed in terms of the experimental bulk elastic constants of Al_3Sc. For both orientations, the bulk Al_3Sc elastic constants[22,23] predict strains of 2.1%. (The similarity of the elasticity predictions for the two orientations results from the small anisotropy of the Al_3Sc elastic constants.) This is a good level of agreement since the magnitudes of the strains are a few percent, so that some deviation from the linear-elasticity prediction is to be expected. The close agreement lends credence to the reliability of the electronic-structure calculations in this case.

The Al/Al_3Sc interfacial energy is computed by subtracting, from the energy of the system with the array of interfaces, the average of the energies of pure Al and Al_3Sc (with the out-of-plane distortion due to the Poisson effect resulting from the in-plane coherency strain) computed in the same size cell. This approach should optimize the convergence of the boundary energy with the integration over the Brillouin zone. In all cases, the Brillouin-zone integration was performed with $k_z=0$ where z is the direction normal to the interface. Most of the calculations were performed using 15 symmetry-independent **k** points for the (100) interface and 11 independent points for the (111) interface. Test calculations were performed with larger sampling sets and the interface energies agreed to within 2%.

Unrelaxed interfacial energies were computed by placing the atoms in each phase in their ideal lattice sites and taking the interplanar spacing *between* the two phases to be the average of the interplanar spacing in each of the parent phases. The unrelaxed energies are 201 mJ/m^2 for the (100) interface and 264 mJ/m^2 for the (111) interface. The larger energy for the (111) interface is consistent with expectations from a simple bond-counting approach (see, for example, Ref. 24).

Technically, the in-plane lattice constant for a coherent interface between two semi-infinite phases should be chosen to minimize the total elastic strain energy. Therefore, some calculations were performed to address the sensitivity of the results to the assumption that the lattice constant in the plane of the boundary is that for Al. The calculations for the (100) interface were repeated for the case where the lattice constant is chosen to be that of Al_3Sc and the Al is distorted due to the Poisson effect. In this case the unrelaxed (100) boundary energy is 219 mJ/m^2, i.e., the change in the (100) interfacial energy was less than 10%.

The interfacial energies were also minimized with respect to the atomic degrees of freedom near the interphase boundary. The energy minimization was performed via a steepest descents method using forces computed from the electronic structure calculations. The steepest descent minimization was continued until the forces were on the order of 1 mRy/a_0 (0.026 eV/Å). This is close to the numerical accuracy of the computed forces. The minimized energies are 192 mJ/m^2 for the (100) interface and 226 mJ/m^2 for the (111) interface. A comparison of the unrelaxed and relaxed results shows that atomic relaxations reduce slightly the crystallographic anisotropy of the interfacial energy. The relaxed structures are illustrated in Figs. 2(a) and 2(b). In these figures, the lines indicate the displacement from the original positions magnified by a factor of 10. The largest displacement for the case of the (100) interface is 0.06 Å and for the (111) interface is 0.07 Å. In both cases the largest displacement is by Sc atoms at the interface which move away from the interface, i.e., closer to the Al_3Sc region.

C. Cluster expansion parameters and predictive capabilities

In order to assess the accuracy of the cluster expansion for the purposes of the present study we performed two tests comparing the predictions of Eq. (1) with the results of direct pseudopotential calculations for the values of Al/Al_3Sc zero-temperature interfacial energies and the Sc heat of solution $[\Delta E(\mathrm{Sc})]$. The cluster expansion was viewed to be sufficiently accurate when the level of agreement was roughly within the accuracy of the pseudopotential calculations. The requirement that the Sc heat of solution is well represented is important because this quantity plays an important role in determining the temperature scale for the solvus boundary, as discussed below.

In Fig. 3 the predictions of the cluster expansion for the interfacial energies and the Sc heat of solution are plotted for various sets of ECI's. It should be emphasized that the cluster-expansion results shown in this figure are *predictions*: The parameters in each cluster expansion were obtained by fitting to the energies of only the 20 small-unit-cell structures listed in Table I; no information about the interfacial energies or Sc heat of solution was directly included in the fitting procedure. Results are shown in Fig. 3 for four different cluster expansions. In cluster expansion (1) ECI's were considered for clusters spanning at most the distance of the second neighbor and containing at most four points. In (2) pair interactions out to fourth neighbor were considered, while triplet and four-body interactions were again within the range of the second neighbor. In (3) the same set of three and four-body interactions was included, but pair ECI's out to eighth neighbor were taken into account. Finally, cluster expansion (4) featured the largest set of ECI's including pairs out to eighth neighbor, triplets with a range out to fourth neighbor, and four-body clusters within the range of the second neighbor. The number of parameters in cluster expansions (1)–(4) (including the ''empty'' and point clusters) was 9, 11, 15, and 17, respectively. The maximum error made in the fit to the 20 values of ΔE listed in Table I was 0.065 and 0.064 eV/atom for cluster expansions (1) and (2), respectively, and 0.024 eV/atom for both (3) and (4). The root-mean-square errors in the fit were considerably smaller, ranging from 0.034 eV/atom for cluster expansion (1) to only 0.009 eV/atom for (4).

The directly calculated values of γ and $\Delta E(\mathrm{Sc})$ plotted with horizontal lines in Fig. 3 were computed with the same

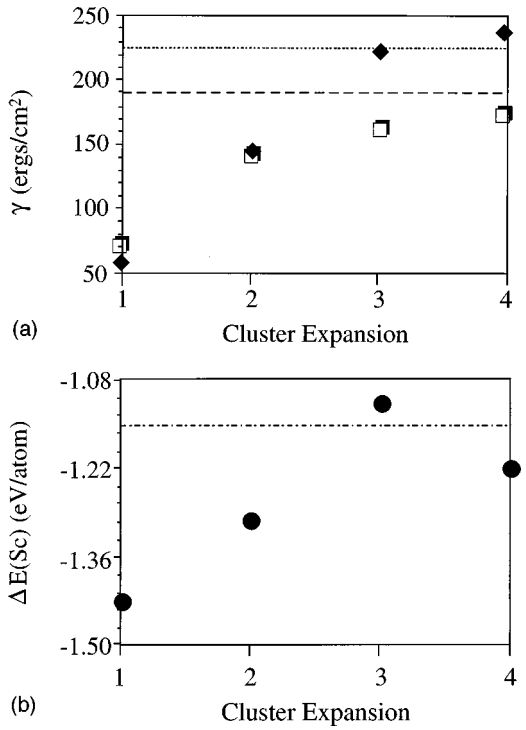

FIG. 3. Comparison of cluster-expansion predictions to directly calculated values of the interfacial energies (a) and Sc heat of solution (b). In (a) directly calculated results for {100} and {111} interfaces are indicated by the horizontal dashed and dotted lines, respectively. The directly calculated value of the Sc heat of solution is indicated in (b) by the horizontal dash-dotted line. Cluster-expansion predictions are denoted by open squares in (a) for {100} and {111} interfacial energies, respectively, and by filled circles in (b) for the Sc heat of solution. The sets of cluster interaction parameters included in each cluster expansion, (1)–(4), are discussed in the text.

pseudopotential approach as was used to compute the fcc superstructure energies from which the ECI's were derived (Table I). The directly calculated value of the Sc heat of solution was computed using 27, 64, and 125 atom supercells where Sc atoms were separated by, respectively, 3, 4, and 5 times the fcc nearest-neighbor spacing. The internal coordinates and volume were fully relaxed for each supercell for the 27 and 64 atom cells. For the 125 atom cell, the energy associated with relaxation was assumed to be equal to that for the 64 atom cell. The calculated values of the Sc heat of solution are estimated to be converged with respect to **k** points to within 0.01 eV/atom at each size. This required 60 independent **k** points for the 27 atom cell, 28 independent points for the 64 atom cell, and 10 independent points for the 125 atom cell. The results are also well converged with respect to system size. The value of $\Delta E(\mathrm{Sc})$ changed by 0.19 eV upon going from the 27 atom to the 64 atom cell but changed by only 0.03 eV going from the 64 to the 125 atom cell. The significant difference between the relaxed impurity energies calculated with 27 and 64 atom cells was also found for unrelaxed values of $\Delta E(\mathrm{Sc})$; this result indicates that the chemical interactions are relatively long ranged. In particular, our results indicate that Sc impurities still interact appreciably when separated by three nearest-neighbor spacings (2.12 lattice spacings in the 27-atom supercell). As was done

TABLE II. Comparison of pseudopotential (PP) and full-potential-linear-augmented-plane-wave (FLAPW) calculated atomic volumes (V) and structural energy differences (ΔE) for elemental Al and Sc. Energies are listed in eV/atom and volumes in Å^3/atom.

	ΔE (PP)	ΔE (FLAPW)	V (PP)	V (FLAPW)
Al fcc	0.0	0.0	15.5	15.9
Al bcc	0.11	0.10	15.9	16.5
Al hcp	0.03	0.04	15.6	16.1
Sc fcc	0.0	0.0	22.8	22.4
Sc bcc	0.05	0.08	23.1	22.8
Sc hcp	−0.05	−0.04	22.9	22.5

for the energies listed in Tables I and II, $\Delta E(\mathrm{Sc})$ was referenced to the fcc phases of both Al and Sc in our calculations.

Figures 3(a) and 3(b) show that eighth-neighbor pair ECI's are required to reproduce accurately the directly calculated values of γ for both {100} and {111} orientations, as well as $\Delta E(\mathrm{Sc})$. The first two cluster expansions not only fail to reproduce well the magnitudes of the heat of solution and interfacial energies, they also fail to capture the degree of anisotropy displayed by the directly calculated values of γ_{100} and γ_{111}. A satisfactory level of agreement between the predictions based upon Eq. (1) and the direct calculations is obtained with cluster expansion (4), which is the one that was used to obtain the results presented below.

D. Accuracy of the pseudopotential calculations

In the calculations which produced the results presented in this section, use was made of two standard approximations. First, all calculations were performed within the framework of density-functional theory using the local-density approximation (LDA). Second, a pseudopotential (PP) electronic-structure method was employed as described above. For completeness, the accuracy of the pseudopotential approach for Sc should be investigated due to the presence of relatively shallow $3p$ core states. We therefore performed several tests comparing results for structural energy differences obtained with the PP and FLAPW methods. The FLAPW method represents a state-of-the-art electronic-structure approach which can be used to obtain the precise LDA result. Therefore, differences between PP and FLAPW calculations should be viewed as being manifestations of inaccuracies introduced by the pseudopotentials.

In Table II we list FLAPW and PP calculated values of the structural energy differences and atomic volumes for fcc, hcp, and bcc phases of elemental Al and Sc. The energy for each structure was optimized with respect to all crystallographic degrees of freedom (volume for fcc and bcc, volume and the c/a ratio for hcp). The energies are relative to the fcc phase as for the results presented in Table I. For Al the structural energy differences calculated by the PP and FLAPW methods are in very good agreement (within 0.010 eV/atom). For Sc the level of agreement between PP and FLAPW calculated structural energy differences is not quite as good. In particular, the fcc-bcc energy difference is underestimated by 0.030 eV/atom in the PP calculations. The atomic volumes calculated with the PP method are roughly

TABLE III. Excess energies (E_{xs}), in eV/atom, for some fcc superstructures containing four-atom and eight-atom unit cells calculated by pseudopotential (PP) and full-potential-linear-augmented-plane-wave (FLAPW) methods. The definition of E_{xs} for each structure is described in the text.

Structure	E_{xs} (PP)	E_{xs} (FLAPW)
IPB-8	0.48	0.45
IMP-8	−1.49	−1.72
Al_3Sc; $L1_2$	−0.48	−0.53

3% smaller compared to the FLAPW results; this is due to the neglect of the so-called ''core corrections'' [25] in the PP calculations.

In Table III we list values of the excess energies (E_{xs}) calculated for three fcc-based superstructures which will be referred to as IPB-8, IMP-8, and $L1_2$ Al_3Sc. The IPB-8 structure mimics the type of supercells used in the calculation of the (100) Al/Al_3Sc interfacial energy; this eight-atom cell is comprised of an fcc Al cube stacked on top of an $L1_2$ Al_3Sc unit cell. The excess energy for the IPB-8 cell is defined as $E_{xs}=8E(\text{IPB-8})-4E(Al_3Sc)-4E(Al)$, where $E(\text{IPB-8})$ is the energy per atom of the IPB-8 structure calculated with all atoms residing on an ideal fcc lattice with a lattice parameter corresponding to bulk Al; $E(Al_3Sc)$ and $E(Al)$ are the energies per atom of $L1_2$ Al_3Sc and fcc Al, respectively, both calculated at the equilibrium Al lattice constant. The IMP-8 structure mimics the type of supercells used in the calculation of the Sc-impurity heat of solution. The lattice vectors for this fcc superstructure are defined as twice those of a primitive fcc unit cell; a Sc atom is placed at the origin of the cell giving an overall composition of Al_7Sc. For the IMP-8 structure the excess energy is defined as $E_{xs}=8E(\text{IMP-8})-7E(Al)-E(Sc)$, where $E(\text{IMP-8})$ is the energy per atom of the IMP-8 (Al_7Sc) structure with all atoms residing on the sites on an undistorted fcc lattice having a lattice parameter corresponding to bulk Al; $E(Al)$ and $E(Sc)$ are the energies per atom of fcc Al and fcc Sc at their own equilibrium lattice parameters. For the $L1_2$ Al_3Sc compound E_{xs} is simply equal to the formation energy per atom (ΔE) as listed in the second column of Table I.

For the IPB-8 structure we find very reasonable agreement between the PP and FLAPW results, suggesting that errors introduced by the use of the PP method in our calculations of the Al/Al_3Sc interfacial energies are likely to be relatively small. For the IMP-8 and $L1_2$ Al_3Sc structures the level of agreement between FLAPW and PP results is not as good, with the FLAPW values being more negative. For the IMP-8 structure the FLAPW-calculated E_{xs} is 0.23 eV more negative than the PP value. This suggests that the true LDA value for the Sc heat of solution [$\Delta E(Sc)$] may be more negative than that calculated by the PP method by roughly 15%. For the $L1_2$ Al_3Sc structure we find a 0.05 eV/atom discrepancy between FLAPW and PP values of $E_{xs}=\Delta E$. In the next section the effect which the discrepancies between FLAPW and PP calculations have upon the calculated bulk and thermodynamic properties will be assessed and it will be argued that they are not significantly important.

IV. THERMODYNAMIC PROPERTIES

A. Solid solubility limits

In order to calculate finite-temperature values of the interfacial energy it is required that the terms $\Delta\mu_0$ and Ω_0 (see Sec. II above) be computed corresponding to the bulk Al and Al_3Sc phases in chemical equilibrium. In the process of performing the calculations of these quantities, the equilibrium phase boundaries for the Al and Al_3Sc phases are derived. The cluster-expansion-LTE-calculated Al solvus is plotted in Fig. 4 where experimentally measured solubility limits are also shown.[26–29] The temperature scales corresponding to the calculated and experimentally measured solubility limits are in rather poor agreement, with the former being roughly 50% too large.

It is important to understand the origin of this discrepancy between the calculated results and experiment. If the Al_3Sc phase is treated as a line compound and the solid solution phase is treated as dilute, then the phase boundary between the bulk Al and Al_3Sc phases is given by the expression

$$c_s(T)=\exp\left[\frac{4\Delta G(Al_3Sc)-\Delta G(Sc)}{k_BT}\right]=\exp\left[\frac{\Delta S(Sc)-4\Delta S(Al_3Sc)}{k_B}\right]\times\exp\left[\frac{4\Delta H(Al_3Sc)-\Delta H(Sc)}{k_BT}\right], \quad (3)$$

where $c_s(T)$ is the solid-solubility limit for Sc in fcc Al, $\Delta G(Al_3Sc)$ is the temperature-dependent formation free energy of the Al_3Sc phase, and $\Delta G(Sc)$ is the free energy associated with the formation of an isolated Sc impurity, *excluding the configurational entropy term*. The ΔH and ΔS terms in Eq. (3) correspond to the enthalpy and entropy contributions to Gibbs free energies $\Delta G(Al_3Sc)$ and $\Delta G(Sc)$. The accuracy of the above equation for the Al/Al_3Sc phase boundary was assessed by comparing the *ab initio* values of $c_s(T)$ calculated from Eq. (3) with those computed using the more accurate LTE technique; an excellent level of agreement was found from $T=0$ K to $T=1500$ K, indicating that the dilute-solution and line-compound approximations are highly accurate in this temperature range. From Eq. (3) it is easy to show that the variation of the solubility limit with temperature is given by

$$\frac{\partial \ln c_s(T)}{\partial(1/T)}=4\Delta H(Al_3Sc)-\Delta H(Sc). \quad (4)$$

The quantity $\{4\Delta H(Al_3Sc)-\Delta H(Sc)\}$ has been obtained from experimental measurements at temperatures near the melting point. The values of −0.61 and −0.72 eV were reported by Fujikawa *et al.*[28] and Hatch,[29] respectively. The PP excess energies calculated in the current work yield a value of $\{4\Delta H(Al_3Sc)-\Delta H(Sc)\}=-0.75$ eV at zero temperature, in excellent agreement with the value of Hatch and in very reasonable agreement with the measurements of Fujikawa *et al.* A value for the *entropy* difference $\{\Delta S(Sc)-4\Delta S(Al_3Sc)\}=1.4k_B$ was also obtained by Fujikawa *et al.* from a fit to Eq. (3) of their measured solubility limits versus $1/T$.

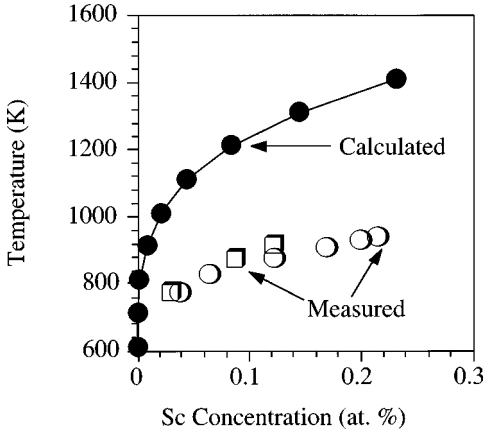

FIG. 4. Calculated and experimentally measured solubility limits for Sc in the Al solid-solution phase. The calculated values are denoted by filled circles, while the open circles and squares denote measured solubility limits taken from Refs. 26–29.

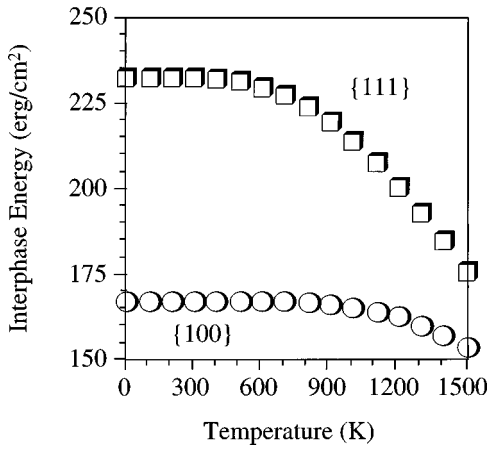

FIG. 5. Calculated interfacial free energies for Al/Al_3Sc interphase boundaries with {111} and {100} orientations are plotted as a function of temperature with open square and circle symbols, respectively.

The discrepancy between the computed solubility limits and the experimentally measured values shown in Fig. 4 can be largely attributed to errors associated with the approximations used in our calculations of thermodynamic properties. In our calculations, the only entropy contribution considered is that associated with configurational disorder. All other sources of entropy, such as atomic vibrations or electronic excitations, are ignored. These ''nonconfigurational'' entropic contributions to $\Delta G(Al_3Sc)$ and $\Delta G(Sc)$ add a prefactor in the relationship between c_s and T [see Eq. (3)] which is neglected in our calculations [i.e., we assume that $\{\Delta S(Sc)-4\Delta S(Al_3Sc)\}$ in Eq. (3) is zero]. The calculated solubility at 950 K is roughly a factor of 10 too small compared with experimental measurements. According to the results of Fujikawa *et al.*, roughly half of this factor can be attributed to the entropy term in Eq. (3) which is neglected in our work; the other half is then due to the difference between the calculated and measured values for the enthalpy difference $\{4\Delta H(Al_3Sc)-\Delta H(Sc)\}$. The value of $\{4\Delta H(Al_3Sc)-\Delta H(Sc)\}$ assessed by Hatch is larger in magnitude and it agrees very well with our calculations. The assessment of Hatch therefore suggests that the magnitude of $\{\Delta S(Sc)-4\Delta S(Al_3Sc)\}$ is even larger than the estimate of Fujikawa *et al.*, and that the entropy prefactor is almost entirely responsible for resolving the discrepancy between the calculated and measured solubility limits.

In light of the discrepancies between FLAPW and PP calculations discussed in Sec. III D, it is important to consider further the agreement between experiment and theory for the enthalpy difference $\{4\Delta H(Al_3Sc)-\Delta H(Sc)\}$ which is important for determining the bulk solid-solubility limits. The errors associated with the use of pseudopotentials in the calculation of this enthalpy difference can be estimated by comparing the PP and FLAPW results for the following quantity: $4E_{xs}(Al_3Sc;L1_2)-E_{xs}(\text{IMP-8})$ (see Sec. III D). The value from the FLAPW method is roughly 8% less negative than that from the PP calculations. If the magnitude of $\{4\Delta H(Al_3Sc)-\Delta H(Sc)\}$ obtained with pseudopotentials is reduced by 8%, the value of this enthalpy difference would lie between the experimental estimates due to Fujikawa *et al.* and Hatch. Therefore, it appears that even if the errors associated with the PP approach are taken into account in the energetics, the discrepancy between the calculated and measured solubility limits must be largely due to the effect of nonconfigurational contributions to the entropy. The measurements and assessments of Hatch and Fujikawa *et al.* clearly indicate that in order to obtain a quantitative description of the solubility limits in this system, it is necessary to consider nonconfigurational contributions to the entropy such as those associated with atomic vibrations.

B. Coherent Al/Al_3Sc interfaces

In order to assess the effect upon interfacial thermodynamic properties resulting from configurational disordering near coherent Al/Al_3Sc interphase boundaries at finite temperature, use was made of the cluster expansion [Eq. (3)] and the LTE approach as outlined in Sec. II. The thermodynamic calculations for fcc-$Al/L1_2$-Al_3Sc interfaces were extended to temperatures beyond the experimentally measured melting point of Al(T_m) in order to estimate the degree of configurational disorder near (100) and (111) interfaces when the calculated bulk solid-solubility limits are roughly equal to those measured experimentally at T_m. Specifically, interfacial free energy calculations were performed for temperatures between 0 and 1500 K.

In Fig. 5 we plot the cluster-expansion-LTE calculated interfacial free energies for (100) and (111) orientations as a function of temperature. As explained above, results are plotted from zero temperature to $T=1500$ K, which is the temperature interval over which the calculated values of $c_s(T)$ span the range of solubilities measured experimentally up the melting point of Al. It can be seen that the effect of temperature is largest for the (111) interfacial free energy. For the (100) orientation the interphase energy is nearly independent of temperature until the bulk solubilities are on the order of 0.1% Sc. By contrast, the (111) interphase energy decreases nearly linearly with T over a wide range of temperatures. The main effect of finite-temperature configurational disordering is seen to be a reduction in the degree of crystallographic anisotropy displayed by the calculated interphase energies.

It is interesting to note that in previous first-principles[30] and semiempirical calculations[31] for coherent Al/Al_3Li inter-

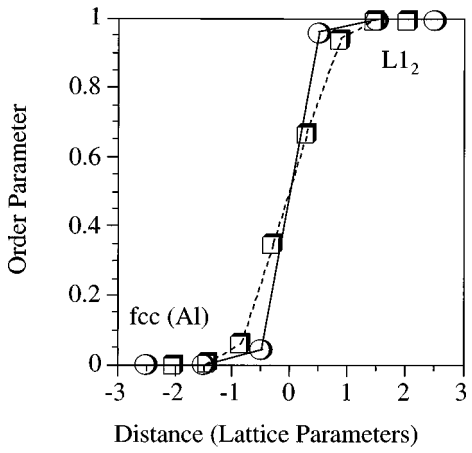

FIG. 6. Calculated order parameters as a function of distance across {111} (open squares) and {100} (open circles) Al/Al_3Sc interfaces at $T=1400$ K. The right-hand (left-hand) side of the figure corresponds to the $L1_2$ Al_3Sc (Al solid-solution) phase. Distances are plotted in units of the average lattice parameter. For {111} orientations the order parameter was defined as the difference between the (Sc) concentration on the Sc and Al sublattice sites on each consecutive plane. For the {100} interface the order parameter was obtained by averaging concentrations over two consecutive planes.

phase boundaries (as is the case for Al/Al_3Sc, the Al/Al_3Li interface is between fcc and $L1_2$ structures), the (111) interphase energy approached $T=0$ K with a finite slope. This is in contrast to what is found in the current calculations for Al/Al_3Sc (111) interphase boundaries (see Fig. 5) where the $d\gamma/dT=0$ at $T=0$ K. The finite slope found in the Al/Al_3Li calculations originates from the use of a cluster expansion containing only ECI's within the range of the second-neighbor pair on the fcc lattice. With such a short-ranged cluster expansion it is found that some of the excitation energies for the (111) interfaces vanish, and a residual excess interfacial entropy results which leads to a finite slope $d\gamma/dT$ at $T=0$ K. This artifact of a short-ranged cluster expansion is removed through the consideration of relatively long-ranged ECI's in the present work.

In Fig. 6 are plotted the results of LTE calculations for the order-parameter profile across (100) and (111) interfaces at $T=1400$ K (where the calculated bulk solubility is $c_s=0.23\%$ Sc, which is roughly the experimentally measured solubility at the melting point of Al). The horizontal axis represents the distance, in lattice parameters, away from the Al/Al_3Sc interface. The order parameter, plotted on the vertical axis, is defined to have values of zero and unity in the solid-solution and perfectly ordered Al_3Sc phases, respectively. It can be seen that the interfaces are predicted to be quite sharp compositionally with the value of the order parameter varying between 0 and 1 within roughly two lattice parameters. Notice that the (111) interphase boundary displays a slightly larger degree of compositional diffuseness, illustrating that for this orientation the interface is slightly more disordered. The larger degree of configurational disorder for the (111) interphase boundary is consistent with the finding that the calculated temperature dependence of the excess free energy is larger for this orientation.

Before concluding this section it is worthwhile to comment about the accuracy of the second-order LTE approach used in the present study. To test the convergence of the LTE, calculations were performed both including and excluding the second-order terms in Eq. (2). For the bulk solubility results plotted in Fig. 4, the difference between the first-order and second-order LTE results was at most 2% of the second-order result. For interphase energies the maximum differences between first and second-order results was 1% for (100) and 9% for (111) at $T=1500$ K. The convergence of the LTE is found to be somewhat poorer for the (111) boundaries which display more configurational disorder. For the LTE-calculated order parameters, the second-order terms gave rise to at most a 2% correction to values calculated in the vicinity of the interphase boundaries. Overall, the contributions of the second-order terms in the LTE were at least an order of magnitude smaller than the first-order contributions, indicating that the expansion was reasonably well converged over the temperature range of interest in this study.

V. SUMMARY AND DISCUSSION

The structural, energetic, and configurational thermodynamic properties of bulk fcc Al-Sc alloys and Al/Al_3Sc interfaces have been calculated from first principles. For (100) and (111) orientations we compute zero-temperature Al/Al_3Sc interfacial energies of 192 and 226 mJ/m^2, respectively. For the range of temperatures considered in this study, chosen in order that the calculated solid-solubilities of Sc in fcc Al span the values measured experimentally up to the melting point of Al, we find that the interfacial free energy decreases much more rapidly with increasing T for the (111) crystallographic orientation. Therefore, an important effect of configurational disordering near the Al/Al_3Sc interphase boundaries is to reduce the degree of anisotropy in the values of the interfacial energy.

The present calculated results for the properties of Al/Al_3Sc interphase boundaries can be compared with those obtained in a prior EAM study by Hyland *et al.*[5] These authors computed zero-temperature values for interfacial energies which were 33, 51, and 78 mJ/m^2, respectively, for {100}, {110}, and {111} orientations. These values are significantly smaller than the presently calculated interfacial energies. Due to the limited amount of experimental data which was available for Al-Sc alloys and which was used in the fitting of the EAM potentials, this result is not surprising. The formation energy of the Al_3Sc phase is computed to be -0.26 eV/atom with the EAM potentials.[5] This value is significantly smaller in magnitude than the LDA results of -0.53 eV/atom obtained here (see Table III). In addition, the ordering energy of the Al_3Sc phase is calculated to be only 0.16 eV/atom using the EAM potentials;[5] this value is again smaller than the current result of 0.29 eV/atom shown in Fig. 1. These comparisons establish the fact that binding of Al and Sc atoms is predicted to be weaker by the EAM potentials in comparison with the LDA results; this finding is consistent with the result that the EAM potentials predict smaller interface energies and more compositional diffuseness near the interphase boundaries at lower temperatures. It should be noted that the relative energies for the different interfacial orientations computed with the EAM suggest that both {110} and {111} interfaces would be unstable with re-

spect to {100} faceting up to temperatures where the precipitates are experimentally observed to be spherical.[1] The current results for the relative interfacial energies of {100} and {111} interphase boundaries suggests substantially less crystallographic anisotropy, and no faceting instability for the {111} orientations. Despite the discrepancies between the previous EAM and present first-principles results, both sets of calculations suggest that configurational disordering gives rise to a weak temperature dependence for the interfacial free energy of the (minimum-free-energy) (100) interphase boundary.

It is interesting to consider a comparison between our calculated values for interfacial energies and the estimate of 94 ± 23 mJ/m^2 obtained by Hyland[1] who used classical nucleation theory to interpret the results of his measured data for precipitation kinetics. Hyland's estimated value is smaller than the numbers obtained in the present study. It is unclear whether this discrepancy is due primarily to inaccuracies introduced by our computational methods, for example due to possible overbinding by the LDA or the neglect of vibrational contributions to the interfacial free energies, or whether it is to some extent attributable to limitations associated with the application of classical nucleation theory in the interpretation of the experimental data. Specifically, for the range of temperatures over which the experimental measurements were performed the critical radius of Al_3Sc precipitates is estimated to be only a few lattice spacings.[5] As discussed by Hyland *et al.*,[5] the critical radius is likely to be comparable to the width of the compositionally diffuse Al/Al_3Sc interface[5] in the range of temperatures considered experimentally and the classical description of the precipitate free energy is therefore of questionable validity.[32] In light of the possible sources or error associated with both the present calculations and Hyland's interpretation of experimental kinetic data, it is important to consider the independent measurement of the interfacial free energy due to Jo and Fujikawa.[33] The values of 40–60 mJ/m^2 obtained by these authors are based upon an analysis of coarsening kinetics using LSW theory.[34–37] In this analysis, a value of the solute diffusivity is required. This value was obtained from an extrapolation from high temperature in the analysis of Jo and Fujikawa. It is possible that such an extrapolation could give rise to significant errors in the estimated interfacial free energies. Given these uncertainties, further experimental work would be desirable.

The current work for Al/Al_3Sc interfaces can be compared to recent semiempirical[31] and first-principles[30] computational studies of the configurational thermodynamic properties for Al/Al_3Li interphase boundaries (as is the case for Al/Al_3Sc, the Al/Al_3Li interphase boundary is also an interface between disordered-fcc and ordered-$L1_2$ structures). In the studies of Asta[31] and Sluiter *et al.*[30] it was found that, compared with Al/Al_3Sc, Al/Al_3Li interfaces were considerably more disordered at temperatures below the melting point of Al. In particular, the width of compositionally diffuse Al/Al_3Li interfaces was estimated to extend between 4 and 5 lattice parameters between 400 and 472 K, compared with less than 2 lattice parameters calculated in the present work at the highest temperatures for Al/Al_3Sc. Furthermore, the finite-temperature corrections to the interfacial energies of Al/Al_3Li interphase boundaries was found to be a much larger fraction of the zero-temperature values of γ. The difference between the interfacial thermodynamic properties for Al/Al_3Sc and Al/Al_3Li can be associated with the much higher degree of long-range order associated with the $L1_2$ phase and the much lower solid-solubility present in the Al solid-solution phase for the Al-Sc system. The comparison between Al/Al_3Li and Al/Al_3Sc illustrates that, in general, the extent to which compositional disorder modifies interfacial thermodynamic properties in substitutional alloys is system dependent; such effects are expected to be most important for interphase boundaries between phases which feature relatively high degrees of compositional disorder.

ACKNOWLEDGMENTS

We are grateful for many helpful discussions with A. J. Ardell, J. J. Hoyt and R. W. Hyland, Jr. We thank Z. W. Lu and Chris Wolverton for assistance with the FLAPW codes, and acknowledge useful suggestions by Alex Zunger. We thank also M. I. Baskes for a critical reading of the manuscript, and D. Gorelikov for providing Ref. 4. This work was supported by the U.S. Department of Energy, Office of Basic Energy Sciences, Materials Science Division, under Contract No. DE-AC04-94AL85000.

*Present address: Materials Science Division, Lawrence Livermore National Lab., P. O. Box 808, L-356, Livermore, CA 94551.

[1] R. W. Hyland, Jr., Metall. Trans. A **23**, 1947 (1992).

[2] J. M. Sanchez, F. Ducastelle, and D. Gratias, Physica A **128**, 334 (1984).

[3] *Pearson's Handbook of Crystallographic Data for Intermetallic Phases*, edited by P. Villars and L. D. Calvert (ASM International, Metals Park, OH, 1991).

[4] A. L. Berezina, V. A. Volkov, B. P. Domashnikov, S. V. Ivanov, and K. V. Chuistov, Metallofizika **12**, 72 (1990); M. E. Dritz and L. B. Ber, Fiz. Met. Metalloved. **57**, 1172 (1984).

[5] R. W. Hyland, Jr., C. L. Rohrer, S. M. Foiles, and M. Asta, Acta Mater. (to be published).

[6] A. A. Quong, S. M. Foiles, and P. D. Tepesch (unpublished).

[7] J. P. Perdew and A. Zunger, Phys. Rev. B **23**, 5048 (1981).

[8] H. J. Monkhorst and J. D. Pack, Phys. Rev. B **13**, 5188 (1976); **16**, 1748 (1977).

[9] A. M. Rappe, K. M. Rabe, E. Kaxiras, and J. D. Joannopoulos, Phys. Rev. B **41**, 1227 (1990).

[10] J. S. Lin, A. Qteish, M. C. Payne, and V. Heine, Phys. Rev. B **47**, 4174 (1993).

[11] N. Troullier and J. L. Martins, Phys. Rev. B **43**, 1993 (1990).

[12] O. K. Anderson, Phys. Rev. B **12**, 3060 (1975); D. R. Hamann, Phys. Rev. Lett. **42**, 662 (1979); E. Wimmer, H. Krakauer, M. Weinert, and A. J. Freeman, Phys. Rev. B **24**, 864 (1981); S.-H. Wei and H. Krakauer, Phys. Rev. Lett. **55**, 1200 (1985); S.-H. Wei, H. Krakauer, and M. Weinert, Phys. Rev. B **32**, 7792 (1985).

[13] D. J. Singh, *Planewaves, Pseudopotentials and the LAPW Method* (Kluwer, Boston, 1994).

[14] D. B. Laks, L. G. Ferreira, S. Froyen, and A. Zunger, Phys. Rev. B **46**, 12 587 (1992).

[15] A. Zunger, in *Statics and Dynamics of Alloy Phase Transformations*, edited by P. E. A. Turchi and A. Gonis, Vol. 319 of *NATO*

Advanced Study Institute, Series B: Physics (Plenum, New York, 1994).
[16] J. W. Cahn, in *Interfacial Segregation*, edited by W. C. Johnson and J. M. Blakely (ASM, Metals Park, Ohio, 1977).
[17] A. F. Kohan, P. D. Tepesch, G. Ceder, and C. Wolverton, Comput. Mater. Sci. **9**, 389 (1998).
[18] F. Ducastelle, *Order and Phase Stability in Alloys* (North-Holland, New York, 1991).
[19] *Binary Alloy Phase Diagrams*, edited by T. B. Massalski, H. Okamoto, P. R. Subramanian, and L. Kacprzak, 2nd ed. (ASM International, Metals Park, OH, 1990).
[20] S. V. Meschel and O. J. Kleppa, in *Metallic Alloys: Experimental and Theoretical Perspectives*, edited by J. S. Faulkner and R. G. Jordan (Kluwer, Netherlands, 1994).
[21] C. J. Sparks, E. D. Specht, G. E. Ice, P. Zschack, and J. Schneibel, in *High Temperature Ordered Intermetalllic Alloys IV*, edited by L. Johnson, D. P. Pope, and J. O. Stiegler, MRS Symposia Proceedings No. 213 (Materials Research Society, Pittsburgh, 1991), p. 363.
[22] R. W. Hyland, Jr. and R. C. Stiffler, Scr. Metall. Mater. **25**, 473 (1991).
[23] E. P. George, J. A. Horton, W. D. Porter, and J. H. Schneibel, J. Mater. Res. **5**, 1639 (1990).
[24] M. Asta, in *Theory and Applications of the Cluster Variation and Path Probability Methods*, edited by J. L. Moran-Lopez and J. M. Sanchez (Plenum, New York, 1996).
[25] S. G. Louie, S. Froyen, and Marvin L. Cohen, Phys. Rev. B **26**, 1738 (1982).
[26] L. A. Willey (unpublished).
[27] M. E. Drits, E. S. Kadaner, T. V. Dobatkina, and N. I. Turkina, Russ. Metall. **4**, 152 (1973).
[28] S. Fujikawa, M. Sugaya, H. Takei, and K. Hirano, J. Less-Common Met. **63**, 87 (1979).
[29] *Aluminum Properties and Physical Metallurgy*, edited by J. E. Hatch (ASM International, Metals Park, OH, 1984).
[30] M. Sluiter and Y. Kawazoe, Phys. Rev. B **54**, 10 381 (1996).
[31] M. Asta, Acta Mater. **44**, 4131 (1996); *Thermodynamics and Kinetics of Phase Transformations*, edited by J. S. Im, B. Park, A. L. Greer, and G. B. Stephenson, MRS Symposia Proceedings No. 398, (Materials Research Society, Pittsburgh, 1996), p. 281.
[32] J. W. Cahn and J. E. Hilliard, J. Chem. Phys. **31**, 688 (1959).
[33] H.-H. Jo and S.-I. Fujikawa, Mater. Sci. Eng. A **171**, 151 (1993).
[34] I. M. Lifshitz and V. V. Slyozov, J. Phys. Chem. Solids **19**, 35 (1961).
[35] C. Wagner, Z. Electrochem. **65**, 581 (1961).
[36] A. J. Ardell, Acta Metall. **20**, 61 (1972).
[37] A. J. Ardell, Acta Metall. **15**, 1772 (1967).